Journal of Alloys and Compounds 850 (2021) 156781

Contents lists available at ScienceDirect

Journal of Alloys and Compounds

journal homepage: http://www.elsevier.com/locate/jalcom

Na^+ diffusivity in carbon-substituted *nido*- and *closo*-hydroborate salts: Pulsed-field-gradient NMR studies of Na-7-$CB_{10}H_{13}$ and $Na_2(CB_9H_{10})(CB_{11}H_{12})$

A.V. Skripov [a, *], G. Majer [b], O.A. Babanova [a], R.V. Skoryunov [a], A.V. Soloninin [a], M. Dimitrievska [c, d], T.J. Udovic [c, e]

[a] Institute of Metal Physics, Ural Branch of the Russian Academy of Sciences, Ekaterinburg, 620108, Russia
[b] Max-Planck-Institute for Intelligent Systems, 70569 Stuttgart, Germany
[c] NIST Center for Neutron Research, National Institute of Standards and Technology, Gaithersburg, MD, 20899-6102, USA
[d] National Renewable Energy Laboratory, Golden, CO, 80401, USA
[e] Department of Materials Science and Engineering, University of Maryland, College Park, MD, 20742, USA

ARTICLE INFO

Article history:
Received 21 April 2020
Accepted 18 August 2020
Available online 23 August 2020

Keywords:
Energy storage materials
Diffusion
Nuclear resonances

ABSTRACT

The mixed-anion solid-solution *closo*-carbahydroborate $Na_2(CB_9H_{10})(CB_{11}H_{12})$ shows the highest room-temperature ionic conductivity among all known solid Na-ion and Li-ion conductors, and the related *nido*-type carbahydroborate Na-7-$CB_{10}H_{13}$ exhibits superionic conductivity above the order-disorder phase transition temperature, ~320 K. To study the Na-ion diffusivity that is closely related to the ionic conductivity in these compounds, we have measured the diffusion coefficients of Na^+ cations in $Na_2(CB_9H_{10})(CB_{11}H_{12})$ and Na-7-$CB_{10}H_{13}$ using the pulsed-field-gradient (PFG) spin-echo technique over the temperature ranges of 298–403 K and 320–403 K, respectively. These measurements have revealed the exceptionally high Na^+ diffusivities (exceeding 2×10^{-6} cm^2/s) for both compounds. In the studied temperature ranges, the diffusion coefficients are found to follow the Arrhenius law with the activation energies of 118(1) meV for $Na_2(CB_9H_{10})(CB_{11}H_{12})$ and 134(3) meV for Na-7-$CB_{10}H_{13}$. For the *nido*-type Na-7-$CB_{10}H_{13}$, the diffusivity results are complemented by the ^1H and ^{23}Na NMR and quasielastic neutron scattering measurements of the atomic jump rates. It is found that the transition from the low-*T* ordered phase to the high-*T* disordered phase occurring near 320 K is accompanied by the abrupt acceleration of both the reorientational jump rate of the $[CB_{10}H_{13}]^-$ anions and the diffusive jump rate of Na^+ cations. For both compounds, a comparison of the measured Na^+ diffusion coefficients with the ionic conductivity results and the data on the cation and anion jump rates provides new insights into unusual dynamical properties of these superionic materials.

1. Introduction

The family of alkali-metal *closo*-hydroborate salts has attracted much recent attention [1], since the disordered phases of some of these salts, such as $Na_2B_{12}H_{12}$, $Na_2B_{10}H_{10}$, $MCB_{11}H_{12}$, and MCB_9H_{10} (M = Li, Na), were found to exhibit extremely high ionic conductivities [2–5]. These compounds are considered as promising solid electrolytes for Li- and Na-ion batteries [6–9]. The characteristic feature of these salts is the occurrence of the order-disorder phase transitions accompanied by abrupt acceleration of both the reorientational (rotational) motion of large *closo*-hydroborate anions and the diffusive motion of metal cations [10–14]. Recent *ab initio* molecular dynamics calculations [15–18] strongly suggest that reorientations of large *closo*-hydroborate anions can facilitate the cation mobility. In most cases, the order-disorder transitions occur above 300 K, so that at room temperature the *closo*-hydroborate salts are in the ordered phase state with low cation mobility. Therefore, for practical applications, it is important to reduce the temperature of the order-disorder phase transition.

One of the possible approaches to reducing this temperature is based on a partial carbon substitution in *closo*-hydroborate anions, when one {B – H} vertex is replaced with {C – H} [4,5]. This carbon substitution leads to the anion valence change from $[B_{12}H_{12}]^{2-}$ or

* Corresponding author.
E-mail address: skripov@imp.uran.ru (A.V. Skripov).

https://doi.org/10.1016/j.jallcom.2020.156781
0925-8388/

$[B_{10}H_{10}]^{2-}$ to $[CB_{11}H_{12}]^{-}$ or $[CB_9H_{10}]^{-}$. Apart from stabilizing the disordered phase state at lower temperatures, this carbon substitution also leads to higher ionic conductivities in the disordered phase [4,5], presumably due to reduced anion − cation Coulombic interactions. Another effective approach to stabilizing the disordered phase state is based on preparing mixed-anion solid solutions. It has been found [19–21] that the order-disorder phase transition is suppressed in mixed-anion solid solutions combining nearly spherical (icosahedral) anions, such as $[B_{12}H_{12}]^{2-}$ or $[CB_{11}H_{12}]^{-}$, and ellipsoidal (bicapped-square-antiprismatic) anions, such as $[B_{10}H_{10}]^{2-}$ or $[CB_9H_{10}]^{-}$. These solid solutions retain the disordered state with high ionic conductivity down to low temperatures. Similar stabilization of the disordered phase was also observed for the mixed-anion solid solution combining the nearly spherical monovalent $[CB_{11}H_{12}]^{-}$ and divalent $[B_{12}H_{12}]^{2-}$ anions, $Na_{2-x}(CB_{11}H_{12})_x(B_{12}H_{12})_{1-x}$ [22].

Recently, investigations of the basic properties of hydroborate salts have been extended to include *nido*-type hydroborates [23]. For *nido*-type anions, one of the regular 12 vertices forming the icosahedral cage of *closo*-type anions is completely removed, so that the resulting nest-like form of *nido* anions contains 11 vertices. It has been found that many properties of sodium *nido*-hydroborates and carbon-substituted *nido*-hydroborates resemble those of the *closo*-type counterparts. In particular, sodium *nido*-hydroborates also exhibit order-disorder phase transitions accompanied by the abrupt increase in ionic conductivity [23] and can also be mixed with sodium *closo*-hydroborates to form highly conductive disordered solid-solution phases [9].

In order to elucidate the mechanisms of ionic conductivity in *closo*- and *nido*-hydroborates, it is important to obtain experimental information both on reorientational motion of the anions and diffusive mobility of the cations. This can be done using nuclear magnetic resonance (NMR), since the measured NMR parameters are sensitive to fluctuations of local magnetic and electric fields arising from atomic jump motion. The usual approach to dynamical NMR studies is based on the measurements of NMR spectra and spin-lattice relaxation rates [24]; this approach can give information on the atomic jump rates over the frequency range of 10^4–10^{11} s^{-1}. However, this approach does not allow to probe cation diffusion coefficients that are closely related to ionic conductivities. The tracer diffusion coefficients can be directly measured using the specialized NMR technique − spin echo with pulsed field gradient (PFG) [25–28]. This method provides a bridge between microscopic and macroscopic measurements of ionic mobility. It is based on observation of an additional attenuation of the spin-echo signal due to displacement of nuclear spins in an external magnetic field gradient. The application of the field gradient serves to set a spatial scale in a certain direction. Combination of direct PFG-NMR measurements of diffusion coefficients with nuclear spin-lattice relaxation measurements of ionic jump rates may allow one to determine the diffusion path. Furthermore, comparison of the measured cation diffusion coefficients with the measured ionic conductivities may clarify the mechanisms of ionic conductivity, including the importance of correlations between the ionic motions. It should be noted that systematic PFG-NMR studies of cation diffusion in complex hydrides are lacking; to the best of our knowledge, the only PFG-NMR measurement in complex hydrides was recently reported for Li^+ diffusion in mixed-anion $Li(CB_9H_{10})_{0.7}(CB_{11}H_{12})_{0.3}$ [7]. PFG-NMR studies of Na^+ diffusion in complex hydrides have not been reported so far.

In the present work, we report the results of ^{23}Na PFG-NMR measurements of sodium diffusion coefficients in two members of the family of superionic conductors based on hydroborate salts: *nido*-Na-7-$CB_{10}H_{13}$ and mixed-anion *closo*-$Na_2(CB_9H_{10})(CB_{11}H_{12})$. The former compound shows the high ionic conductivity (~4×10^{-3} S/cm at 370 K) above the order-disorder phase transition at ~320 K [23]. The corresponding *nido*-type anion 7-$CB_{10}H_{13}^-$ is schematically shown in Fig. 1a. For this compound, sodium diffusivity results are complemented by ^1H and ^{23}Na NMR and quasielastic neutron scattering (QENS) measurements of the atomic jump rates. It should be noted that no dynamical NMR and QENS studies of any *nido*-type hydroborate salts have been reported so far, apart from the neutron-elastic-scattering fixed-window scans [23]. The mixed-anion solid solution $Na_2(CB_9H_{10})(CB_{11}H_{12})$ exhibits the highest room-temperature ionic conductivity (~0.07 S/cm [20]) among all the studied Na-ion and Li-ion conductors. The *closo*-type anions $CB_9H_{10}^-$ and $CB_{11}H_{12}^-$ are schematically represented in Fig. 1b and c. Comparison of the measured sodium diffusion coefficients

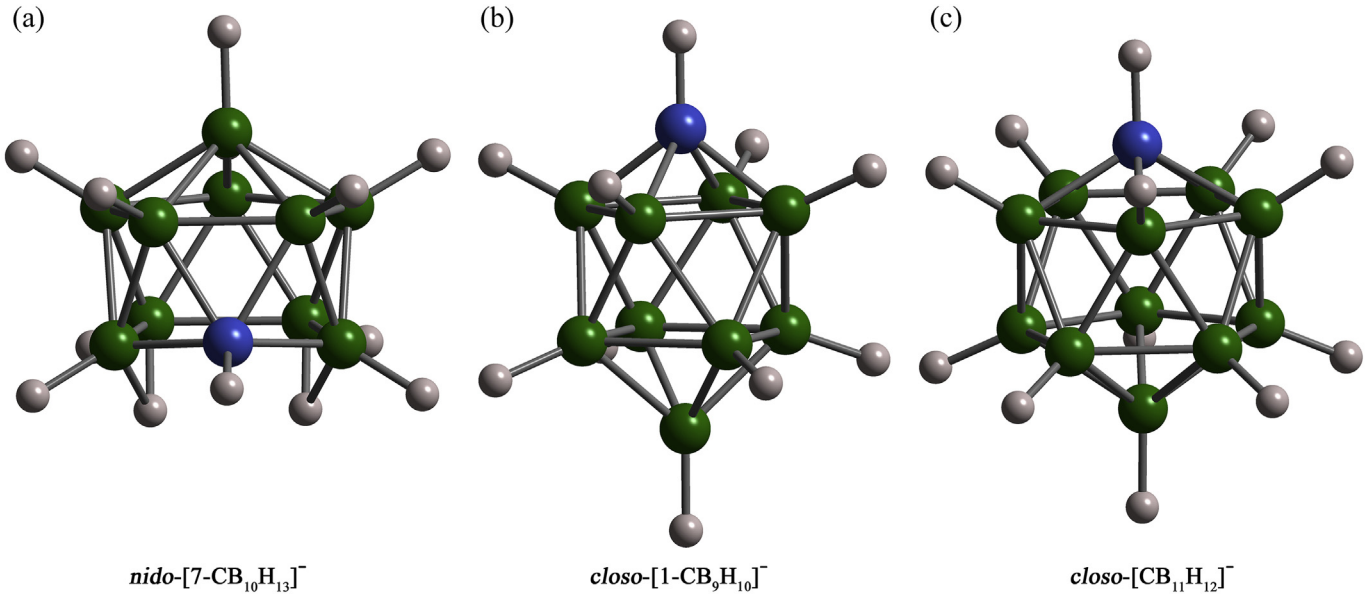

Fig. 1. Schematic view of the nest-like 7-$CB_{10}H_{13}^-$ anion (a), the bicapped-square-antiprismatic $CB_9H_{10}^-$ anion (b), and the icosahedral $CB_{11}H_{12}^-$ anion (c). Green spheres: B atoms, blue spheres: C atoms, and gray spheres: H atoms. (For interpretation of the references to colour in this figure legend, the reader is referred to the Web version of this article.)

for $Na_2(CB_9H_{10})(CB_{11}H_{12})$ with the ionic conductivity results [20] and the data on the cation and anion jump rates [29] provides new insights into the mechanism of superionic conduction in this unique material.

2. Experimental details

Sodium monocarba-*nido*-undecaborate Na-7-$CB_{10}H_{13}$ was obtained from Katchem [30]. Residual water was removed by annealing at 393 K for 16 h under vacuum. According to X-ray diffraction analysis [23], the room-temperature ordered phase of Na-7-$CB_{10}H_{13}$ is orthorhombic (space group $Pna2_1$) with the lattice parameters $a = 10.9919(4)$ Å, $b = 11.6564(5)$ Å, and $c = 7.1720(4)$, and the disordered phase is cubic ($Fm\text{-}3m$) with the lattice parameter $a = 9.983(2)$ Å at 370 K. The mixed-anion solid solution $Na_2(CB_9H_{10})(CB_{11}H_{12})$ was prepared by drying the aqueous solution of equimolar amounts of $NaCB_9H_{10}$ and $NaCB_{11}H_{12}$ (obtained from Katchem), as described in Ref. 20. According to X-ray diffraction analysis, the dominant phase of $Na_2(CB_9H_{10})(CB_{11}H_{12})$ has the hexagonal close-packed structure with the lattice parameters $a = 6.991(1)$ Å and $c = 11.339(2)$ Å. This phase is isomorphous to that found for the pristine superionic $NaCB_9H_{10}$ above ~310 K [5], but has a slightly larger unit cell. The presence of a second trace solid-solution phase of $Na_2(CB_9H_{10})(CB_{11}H_{12})$ (<1 mol.%) corresponds to face-centered-cubic polymorphic packing.

For NMR experiments, the samples were flame-sealed in glass tubes under vacuum. NMR measurements of the spectra and spin-lattice relaxation rates were performed on a pulse spectrometer with quadrature phase detection at the frequencies $\omega/2\pi = 14$ and 27 MHz (^{1}H) and 23 MHz (^{23}Na). The magnetic field was provided by a 2.1 T iron-core Bruker magnet. A home-built multinuclear continuous-wave NMR magnetometer working in the range 0.32–2.15 T was used for field stabilization. For rf pulse generation, we used a home-built computer-controlled pulse programmer, the PTS frequency synthesizer (Programmed Test Sources, Inc.), and a 1 kW Kalmus wideband pulse amplifier. Typical values of the $\pi/2$ pulse length were 2–3 μs for both ^{1}H and ^{23}Na. A probehead with the sample was placed into an Oxford Instruments CF1200 continuous-flow cryostat using nitrogen as a cooling agent. The sample temperature, monitored by a chromel-(Au–Fe) thermocouple, was stable to ±0.1 K. The nuclear spin-lattice relaxation rates were measured using the saturation–recovery method. NMR spectra were recorded by Fourier transforming the solid echo signals (pulse sequence $\pi/2_x - t - \pi/2_y$).

Pulsed-field-gradient NMR (PFG-NMR) measurements of Na^+ diffusion coefficients were performed on a Bruker AVANCE III 400 spectrometer operating at the resonance frequency of 105.8 MHz. Magnetic field gradients were generated by a diff60 diffusion probe and a Great60 gradient amplifier (Bruker Biospin). All diffusivities were measured using the Hahn spin-echo sequence with spoiler gradients [31]. The shape of the gradient pulses was given by a half-sine function with a length of δ_{sine}, which corresponds to the effective gradient pulse length of $\delta_g = (2/\pi)\delta_{sine}$. The diffusion coefficients were deduced from the decrease in the integrated intensity of Fourier-transformed spin-echo with increasing amplitude of the applied field-gradient pulses g. The diffusion time Δ between two gradient pulses of the pulse sequence was fixed at 3 ms, and their effective length δ_g was 1 ms. It should be noted that the choice of the pulse sequence and gradient pulse parameters was determined by the short ^{23}Na spin-lattice relaxation times in our samples (of the order of a few milliseconds). The amplitude of the gradient pulses g was varied in 16 steps up to 2.4 kG/cm.

Quasielastic neutron scattering experiments were performed at the National Institute of Standards and Technology (NIST) Center for Neutron Research on the Disk Chopper Spectrometer (DCS) [32] utilizing an incident neutron wavelength of 9 Å. The energy resolution was 22 μeV (full width at half-maximum), and the maximum attainable Q value was about 1.31 Å^{-1}. The instrumental resolution function was determined from the measured QENS spectrum at 100 K.

For all figures, standard uncertainties are commensurate with the observed scatter in the data, if not explicitly designated by vertical error bars.

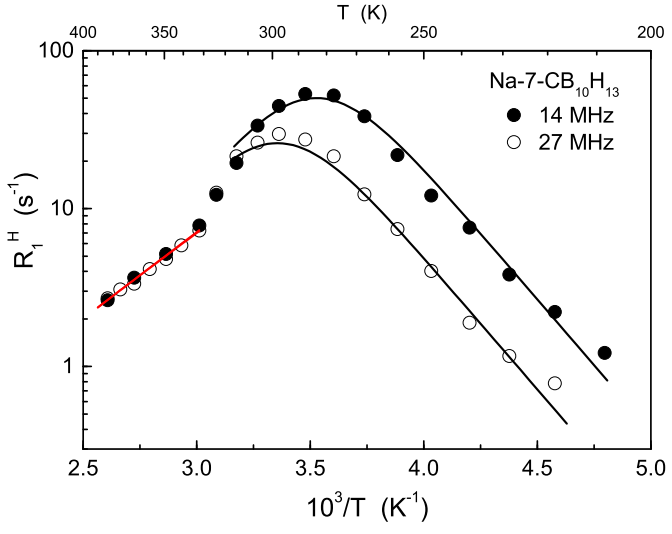

Fig. 2. Proton spin-lattice relaxation rates measured at 14 and 27 MHz for Na-7-$CB_{10}H_{13}$ as functions of the inverse temperature. The black solid lines show the simultaneous fit of the standard model to the data for the ordered phase over the temperature range 209–315 K. The red solid line shows the fit of the standard model to the data for the disordered phase over the temperature range 332–384 K. (For interpretation of the references to colour in this figure legend, the reader is referred to the Web version of this article.)

3. Results and discussion

3.1. Anion and cation jump rates in Na-7-$CB_{10}H_{13}$: NMR and QENS results

The temperature dependence of the proton spin-lattice relaxation rate R_1^H for Na-7-$CB_{10}H_{13}$ measured at two resonance frequencies $\omega/2\pi$ is shown in Fig. 2. As can be seen from this figure, $R_1^H(T)$ exhibits a frequency-dependent maximum that is typical of the spin-lattice relaxation mechanism due to motionally-modulated dipole-dipole interactions between nuclear spins [33]. This maximum is expected to occur at the temperature at which the proton jump rate τ_H^{-1} becomes nearly equal to the resonance frequency ω. As in the other borohydrides and related compounds [24], this proton jump rate is associated with reorientations of H-containing anions.

According to the standard theory of nuclear spin-lattice relaxation due to the motionally-modulated dipole-dipole interaction [33], in the limit of slow motion ($\omega\tau_H \gg 1$), R_1^H should be proportional to $\omega^{-2}\tau_H^{-1}$, and in the limit of fast motion ($\omega\tau_H \ll 1$), R_1^H should be proportional to τ_H, being frequency-independent. If the temperature dependence of the proton jump rate follows the Arrhenius law,

$$\tau_H^{-1} = \tau_{H0}^{-1} \exp(-E_a / k_B T) \quad (1)$$

with the activation energy E_a for the reorientational motion, the

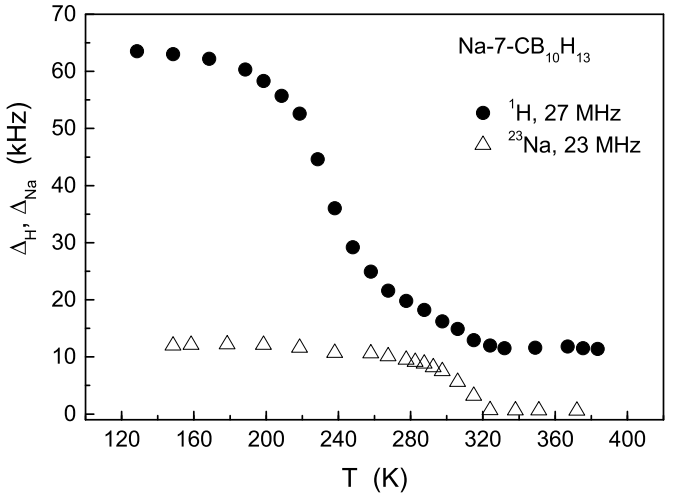

Fig. 3. Temperature dependence of the width (full width at half-maximum) of the ^{1}H and ^{23}Na NMR spectra for Na-7-$CB_{10}H_{13}$.

plot of ln R_1^H versus T^{-1} is expected to be linear in the limits of both slow and fast motion with the slopes of $-E_a/k_B$ and E_a/k_B, respectively. The behavior of $R_1^H(T)$ in the range 315–330 K (see Fig. 2) strongly deviates from the predictions of the standard theory. Indeed, the sharp drop of the relaxation rate in this range indicates the occurrence of an order-disorder phase transition accompanied by an abrupt acceleration of the anion reorientations. Similar behavior of $R_1^H(T)$ was observed near the order-disorder phase transitions in a number of *closo*-hydroborate systems [10,11,13]. According to the differential scanning calorimetry (DSC) measurements [23] performed at the heating and cooling rates of 20 K/min, the order-disorder phase transition in Na-7-$CB_{10}H_{13}$ occurs near 333 K (heating) and 305 K (cooling). It should be noted that all NMR measurements described in this section were performed with increasing temperature and with 15 min stabilization time at each temperature prior to a measurement.

Because of the strong changes in the motional parameters of anion reorientations at the phase transition point, the experimental $R_1^H(T)$ data should be separately analyzed for the low-temperature (ordered) phase and the high-temperature (disordered) phase. For the ordered phase, the straightforward approach includes a combination of the Arrhenius law (Equation (1)) and the standard expression that relates R_1^H with τ_H^{-1} (see Supplementary Information). The parameters of this model are the activation energy E_a, the pre-exponential factor τ_{H0} of the Arrhenius law, and the amplitude factor ΔM_H determined by the strength of the fluctuating part of dipole-dipole interactions. These parameters have been varied to find the best fit to the $R_1^H(T)$ data at two resonance frequencies *simultaneously*. The results of the simultaneous fit for the ordered phase over the T range of 209–315 K are shown by black solid lines in Fig. 2; the corresponding fit parameters are E_a = 330(20) meV, τ_{H0} = 1.5(1) × 10^{-14} s, and $\Delta M_H = 1.4(1) \times 10^9$ s^{-2}.

For the disordered (high-temperature) phase, only the activation energy can be directly obtained from the experimental $R_1^H(T)$ data, since the relaxation rate maximum is not reached for this phase. The value of the activation energy determined from the slope of the ln R_1^H vs. T^{-1} plot over the temperature range of 332–384 K is 219(5) meV; the corresponding fit is shown by the red solid line in Fig. 2. It should be noted that the activation energy value for anion reorientations in the disordered phase of *nido*-Na-7-$CB_{10}H_{13}$ is close to those found for the disordered phases of *closo*-hydroborates [10,12,13]. In order to estimate the pre-exponential factor τ_{H0} for the disordered phase from the $R_1^H(T)$ data, some additional assumptions are required. A possible approach is based on the assumption that the amplitude factor ΔM_H in the disordered phase is the same as in the ordered phase, since the order-disorder transition only slightly changes the nearest-neighbor distances for H atoms. Using this assumption, we obtain $\tau_{H0} = 3.8(1) \times 10^{-13}$ s from the $R_1^H(T)$ data for the disordered phase.

Measurements of the line width of ^{1}H NMR spectra can probe the anion reorientational motion at a slower frequency scale than the spin-lattice relaxation measurements. The temperature dependence of the ^{1}H NMR line width Δ_H (full width at half-maximum) measured at 27 MHz is shown in Fig. 3. At low temperatures the line width is determined by static dipole-dipole interactions of ^{1}H spins; in our case, this "rigid-lattice" line width Δ_{RL} is about 63 kHz. With increasing temperature, the observed line width decreases due to a partial averaging of the dipole-dipole interactions of ^{1}H spins by atomic jump motion. This motional line narrowing becomes substantial when the jump rate $\tau_H^{-1}(T)$ exceeds Δ_{RL}. For Na-7-$CB_{10}H_{13}$, this happens near 220 K (see Fig. 3). At high temperatures, the measured line width reaches a plateau of about 11 kHz. Such a high-temperature line width plateau is the typical feature of borohydrides and related compounds [24]. It originates from the fact that reorientations cannot completely average out the dipole-dipole interactions even in the case when $\tau_H^{-1} \gg \Delta_{RL}$; indeed, "intermolecular" dipolar interactions (between nuclear spins belonging to different reorienting groups) are not fully averaged by the localized (reorientational) motion. Since the line width plateau regime is already reached near the order-disorder transition temperature, we do not observe any considerable changes of Δ_H in the transition region (see Fig. 3), in spite of the strong changes in τ_H^{-1}.

Information on the anion reorientational motion can also be obtained from quasielastic neutron scattering measurements. Because of the huge incoherent neutron scattering cross-section of protons, the observed QENS spectra for complex hydrides are

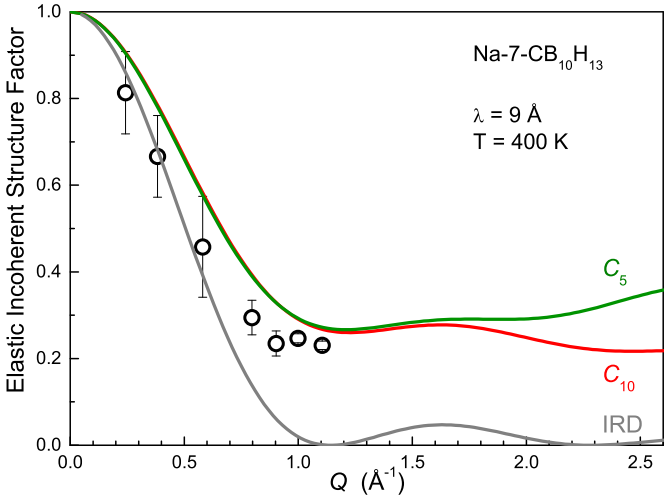

Fig. 4. The elastic incoherent structure factor for $CB_{10}H_{13}^-$ anions in Na-7-$CB_{10}H_{13}$ as a function of Q. The experimental points (circles) are determined from the DCS data (using the incident neutron wavelength of 9 Å) at 400 K. The curves represent the model of uniaxial five-fold jumps of the anions (green), the model of uniaxial ten-fold jumps of the anions (red), and the model of isotropic rotational diffusion (gray). (For interpretation of the references to colour in this figure legend, the reader is referred to the Web version of this article.)

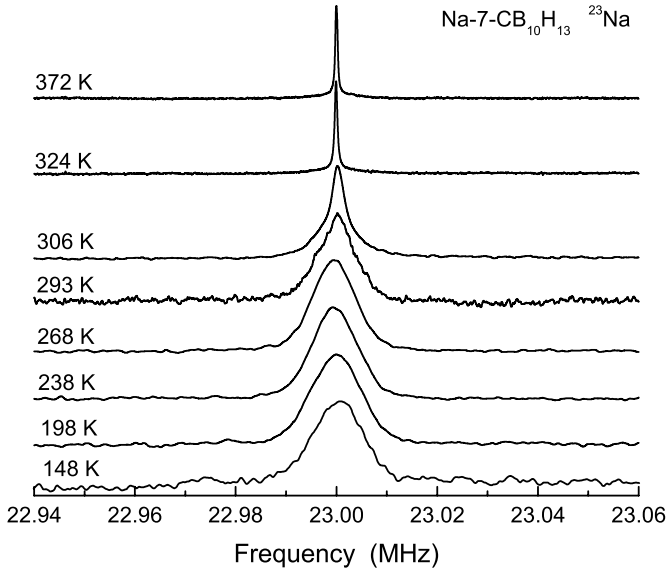

Fig. 5. Evolution of the measured ^{23}Na NMR spectra with temperature for Na-7-$CB_{10}H_{13}$.

strongly dominated by the contribution due to incoherent scattering on ^{1}H nuclei. A representative QENS spectrum for Na-7-$CB_{10}H_{13}$ is shown in Figure S1 of the Supplementary Information. As typical of the case of localized H motion [34,35], this spectrum consists of the narrow elastic line with the width determined by the instrument resolution and the broader quasielastic line with a nearly Q-independent width which is proportional to τ_H^{-1}. It should be noted that the quasielastic line broadening was observed only in the disordered phase of Na-7-$CB_{10}H_{13}$; the energy resolution was not sufficient to probe the slower H motion in the ordered phase. The width (full width at half-maximum) of the quasielastic component is found to change from 18(4) μeV at 330 K to 39(8) μeV at 400 K. Information on the geometry of localized H motion can be obtained from the Q dependence of the elastic incoherent structure factor (EISF) which represents a relative contribution of the elastic line intensity to the total intensity of the QENS spectrum. In Fig. 4, the experimental EISF results at 400 K are compared to the model calculations for three rotational models compatible with the symmetry of the anions. The expressions resulting from these model calculations are included in the Supplementary Information. The first model (C_5) corresponds to jump reorientations around the five-fold symmetry axis of the boron frame (going through the C − H bond of $CB_{10}H_{13}^-$). This choice of the axis is based on *ab initio* molecular dynamics calculations [18] for $NaCB_{11}H_{12}$, showing that anion rotations around the five-fold axis going through the C − H bond are preferable due to the abnormally high positive Mulliken charge on the C-bound H atom [4]. For $CB_{10}H_{13}^-$, Mulliken charge calculations also indicate an abnormally high positive charge on the C-bound H atom [23]. It should be noted, however, that a choice of another five-fold axis would lead to only slight changes in the behavior of the EISF. The second model (C_{10}) mimics the smaller-angle rotations around the same five-fold symmetry axis, and the third model (IRD) corresponds to isotropic rotational diffusion, when all H atoms perform small jumps on the surface of a sphere. In the limited Q range of our measurements, the experimental EISF results appear to be consistent with both C_5 and C_{10} models. It is evident that high-Q measurements are required to further clarify the mechanism of anion reorientations in this *nido*-type compound.

The jump motion of Na^+ cations in Na-7-$CB_{10}H_{13}$ can be probed by ^{23}Na NMR measurements. Fig. 5 shows the evolution of the observed ^{23}Na NMR spectrum with temperature; the temperature dependence of the ^{23}Na NMR line width (full width at half-maximum) is included in Fig. 3. As can be seen from Figs. 3 and 5, in contrast to the case of the proton NMR line showing the high-temperature plateau, the ^{23}Na line becomes very narrow (~0.6 kHz) above 320 K. Such a behavior indicates the onset of a *long-range* diffusion of Na^+ cations at the NMR frequency scale. Fig. 6 shows the measured ^{23}Na spin-lattice relaxation rate R_1^{Na} as a function of the inverse temperature. It can be seen that $R_1^{Na}(T)$ exhibits the Arrhenius-type behavior both at low and high temperatures, as typical of the motionally induced spin-lattice relaxation rate. As in the other sodium hydroborates [3,10,13,29], the measured R_1^{Na} values for Na-7-$CB_{10}H_{13}$ are much higher than those expected for the ^{23}Na − ^{1}H dipole-dipole interaction; therefore, the ^{23}Na spin-lattice relaxation is dominated by fluctuations of the

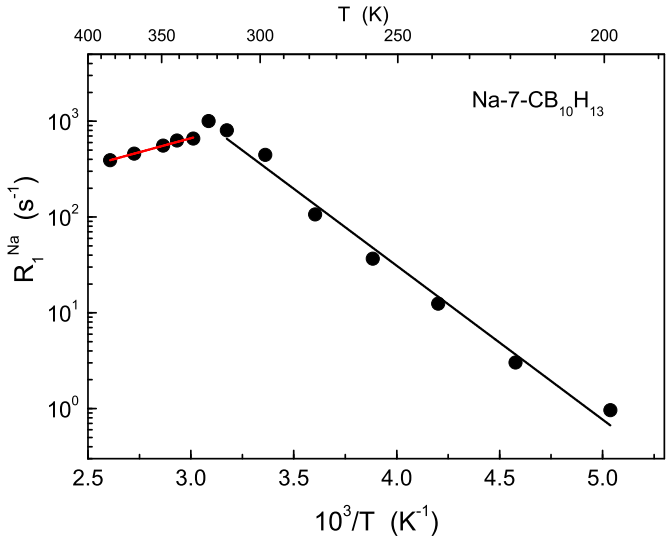

Fig. 6. ^{23}Na spin-lattice relaxation rate measured at 23 MHz for Na-7-$CB_{10}H_{13}$ as a function of the inverse temperature. The black and red lines show the Arrhenius fits to the data for the ordered and disordered phases, respectively. (For interpretation of the references to colour in this figure legend, the reader is referred to the Web version of this article.)

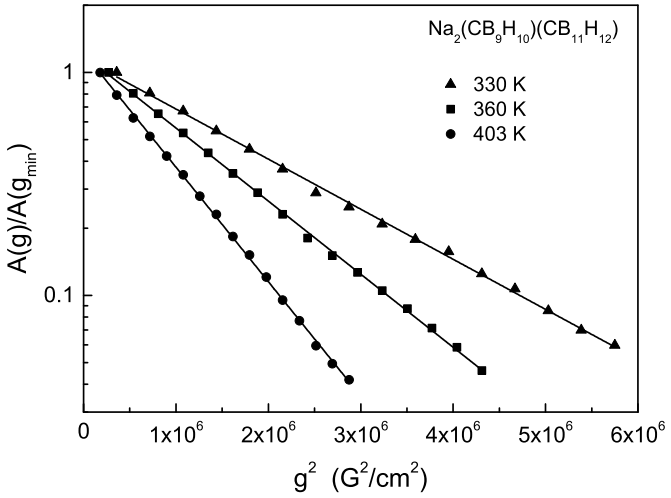

Fig. 7. The ^{23}Na spin-echo attenuation as a function of the square of the effective gradient pulse amplitude for $Na_2(CB_9H_{10})(CB_{11}H_{12})$ at three temperatures. The solid lines show the fits of the exponential function (Equation (2)) to the data.

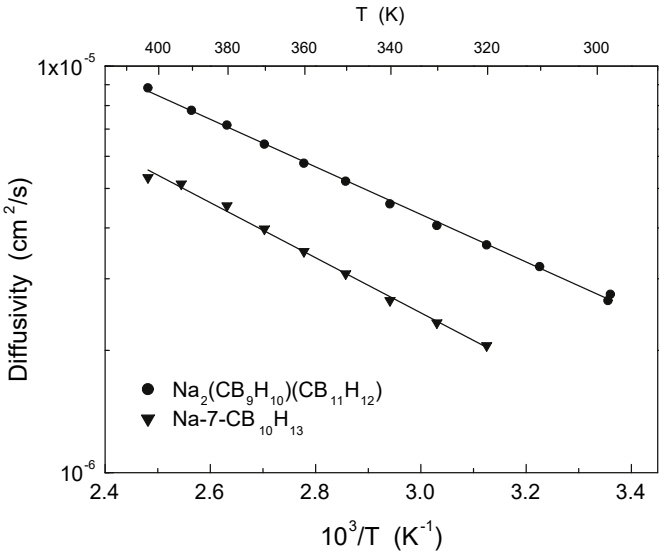

Fig. 8. The measured Na^+ diffusion coefficients for $Na_2(CB_9H_{10})(CB_{11}H_{12})$ and Na-7-$CB_{10}H_{13}$ as functions of the inverse temperature. The solid lines show the Arrhenius fits to the data.

quadrupole interaction resulting from Na^+ jumps. It should be noted that $R_1^{Na}(T)$ does not pass through a regular maximum; instead, the slope of the log R_1^{Na} vs. T^{-1} plot is found to change abruptly near 320 K. Such a behavior can be described as "folding" of the relaxation rate peak [3,10,13]: due to the abrupt change in the Na^+ jump rate τ_{Na}^{-1} at the phase transition point, the relaxation rate jumps directly from the low-temperature slope of the peak to the high-temperature slope. Since a regular maximum of $R_1^{Na}(T)$ is not observed, we can only conclude that in the disordered high-temperature phase τ_{Na}^{-1} exceeds ω ~10^8 s^{-1} and determine the activation energies for Na^+ diffusion in both the ordered and disordered phases. The corresponding estimates from the low-T and high-T slopes of the ^{23}Na spin-lattice relaxation rate give 320(9) meV and 116(7) meV, respectively.

3.2. Na^+ diffusivity in Na-7-$CB_{10}H_{13}$ and $Na_2(CB_9H_{10})(CB_{11}H_{12})$: Pulsed-field-gradient NMR results

The high ^{23}Na spin-lattice relaxation rates (i. e., short spin-lattice relaxation times, of the order of a few milliseconds) in sodium-based complex hydrides strongly restrict the applicability of PFG-NMR to studies of Na^+ diffusion coefficients in this class of compounds. This is probably the main reason why PFG-NMR studies of sodium diffusion in complex hydrides have not been reported so far. In the case of our Na-7-$CB_{10}H_{13}$ and $Na_2(CB_9H_{10})(CB_{11}H_{12})$ compounds, such measurements prove to be feasible due to the extremely high Na^+ diffusivity leading to substantial echo attenuation even for a small diffusion time ($\Delta = 3$ ms). For sinusoidal field-gradient pulses, the diffusion-induced attenuation of the spin-echo intensity A as a function of the pulsed field gradient amplitude g can be written in the form [27,36,37].

$$\frac{A(g)}{A(0)} = \exp\left[-\gamma^2 D \delta_g^2 \left(\Delta - \frac{\pi}{8}\delta_g\right) g^2\right], \qquad (2)$$

where D is the diffusion coefficient, γ is the gyromagnetic ratio for ^{23}Na, and δ_g is the effective gradient pulse length. As an example of the data, Fig. 7 shows the spin-echo attenuation as a function of g^2 for $Na_2(CB_9H_{10})(CB_{11}H_{12})$ at three temperatures. It can be seen that the dependence of the spin-echo amplitude on g^2 is satisfactorily described by Eq. (2). Similar behavior of the spin-echo attenuation was also observed for Na-7-$CB_{10}H_{13}$. The Na^+ diffusion coefficients derived from the spin-echo attenuation for $Na_2(CB_9H_{10})(CB_{11}H_{12})$ and Na-7-$CB_{10}H_{13}$ are shown in Fig. 8 as functions of the inverse temperature. It should be noted that for both compounds, the measured Na^+ diffusivity is more than an order of magnitude higher than the Li^+ diffusivity reported for $Li(CB_9H_{10})_{0.7}(CB_{11}H_{12})_{0.3}$ in the range 298–333 K [7]. As can be seen from Fig. 8, the Na^+ diffusivity exhibits the Arrhenius-type behavior over the ranges of 298–403 K for $Na_2(CB_9H_{10})(CB_{11}H_{12})$ and 320–403 K for Na-7-$CB_{10}H_{13}$; the corresponding activation energies are 118(1) meV and 134(3) meV, respectively. For Na-7-$CB_{10}H_{13}$ the PFG-NMR diffusivity measurements were only possible in the disordered (high-T) phase; in the ordered phase, the values of D were too low to be measured by PFG-NMR with the same set of parameters. This is consistent with the abrupt change of conductivity at the order-disorder phase transition point [23].

As the first step in an analysis of the Na^+ diffusivity results, we have to compare the activation energies obtained from the PFG-NMR experiments with those derived from the high-temperature R_1^{Na} measurements. If there are no changes in the diffusion mechanisms, the temperature dependence of the diffusion coefficient is determined by that of the Na^+ jump rate, and the corresponding activation energies are expected to be the same. For $Na_2(CB_9H_{10})(CB_{11}H_{12})$, the activation energy estimated from the high-T piece of the $R_1^{Na}(T)$ data over the range 330–435 K is 135(8) meV [29]. This value is close to that obtained from PFG-NMR, 118(1) meV. For Na-7-$CB_{10}H_{13}$, the activation energies derived from the high-T R_1^{Na} data and PFG-NMR are also rather close to each other: 116(7) meV and 134(3) meV, respectively. Neglecting any correlations for diffusive jumps, the elementary jump length L can be estimated from the expression $D = L^2\tau_{Na}^{-1}/6$. For $Na_2(CB_9H_{10})(CB_{11}H_{12})$, for such an estimate we can use the value $\tau_{Na}^{-1}(330\ \mathrm{K}) \approx 5 \times 10^9\ s^{-1}$ derived from the R_1^{Na} results [29] and the characteristic value of $D(330\ \mathrm{K}) \approx 4 \times 10^{-6}$ cm^2/s; this yields $L = 6.9$ Å. The estimated L value is larger than the distance between the nearest-neighbor tetrahedral (T) and octahedral (O) interstitial sites in the hexagonal close-packed anion sublattice of $Na_2(CB_9H_{10})(CB_{11}H_{12})$, $d_{TO} = 4.28$ Å [29]. Such a difference may be related to the complex nature of Na^+ diffusive motion in this compound, where the fast localized jumps between closely-spaced T sites are found to coexist with slower jumps between T and O sites [29]. Similar effects are well documented for hydrogen diffusion in Laves-phase hydrides, where the diffusion path includes fast localized H jumps within the hexagons formed by tetrahedral interstitial sites and slower H jumps from one such hexagon to another [38–40]. Another possible reason for the large effective L value may be related to correlations between jumps of different cations adjoining a large anion. Indeed, according to the results of recent *ab initio* calculations for $Li_2B_{12}H_{12}$ and $Na_2B_{12}H_{12}$ [17] and for $LiCB_{11}H_{12}$ and $NaCB_{11}H_{12}$ [18], Li^+ and Na^+ cations surrounding a single $[B_{12}H_{12}]^{2-}$ or $[CB_{11}H_{12}]^-$ anion have some energetically preferable angular configurations; therefore, a rotation of the anion can facilitate jumps of several cations. For Na-7-$CB_{10}H_{13}$, the analogous estimate of L appears to be impossible, since the values of τ_{Na}^{-1} cannot be reliably extracted from the R_1^{Na} data for this compound (see the previous section).

It is interesting to estimate the mean-square displacement $\langle r^2 \rangle$ for Na^+ ions in the course of our diffusivity measurements. For three-dimensional diffusion, the mean-square displacement is known to change with time t as $\langle r^2 \rangle = 6Dt$. Taking the diffusion time of 3 ms and the characteristic value of $D(300\ \mathrm{K}) \approx 2.8 \times 10^{-6}$ cm^2/s

for $Na_2(CB_9H_{10})(CB_{11}H_{12})$, we obtain $\langle r^2 \rangle = 5.0 \times 10^{-8}$ cm^2, i. e., $\langle r^2 \rangle^{1/2} = 2.2 \times 10^{-4}$ cm. Therefore, in our experiments, the diffusion coefficients are probed over the distances of a few microns. This provides a basis for comparison between the diffusivity and ionic conductivity results. Using the measured tracer diffusion coefficient, we can estimate the ionic conductivity σ from the Nernst-Einstein equation

$$\sigma = \frac{nD(Ze)^2}{k_B T}, \quad (3)$$

where n is the number of charge carriers per unit volume and Ze is the electrical charge of the carrier. Using the lattice parameters of $Na_2(CB_9H_{10})(CB_{11}H_{12})$ [20], we find that $n = 4.17 \times 10^{21}$ cm^{-3} and σ(300 K) = 0.073 S/cm. The measured ionic conductivity of $Na_2(CB_9H_{10})(CB_{11}H_{12})$ near 300 K is about 0.07 S/cm [20]. Therefore, for this compound, the experimental Na^+ diffusivity is consistent with the measured ionic conductivity near room temperature. The effects of correlations for the cation diffusive jumps [18] are manifested only in the relation between τ_{Na}^{-1} and the diffusion coefficient (see above).

Because of the order-disorder phase transition in Na-7-$CB_{10}H_{13}$, the Na^+ diffusivity and conductivity for this compound should be compared well above the transition temperature. Using the lattice parameters of the disordered cubic phase of Na-7-$CB_{10}H_{13}$ at 370 K [23], we find that $n = 4.02 \times 10^{21}$ cm^{-3}. Taking the value of D(370 K) $\approx 4 \times 10^{-6}$ cm^2/s, on the basis of the Nernst-Einstein equation we obtain that σ(370 K) $\approx 8 \times 10^{-2}$ S/cm. The measured ionic conductivity of Na-7-$CB_{10}H_{13}$ near 370 K is about an order of magnitude lower (~4×10^{-3} S/cm [23]). In principle, such a discrepancy may be attributed to a presence of some inhomogeneities (at the length scale exceeding a few microns) which are expected to reduce the measured conductivity. It should also be noted that, for both compounds, the activation energies for Na^+ diffusion coefficients appear to be lower than those for the experimental σT product (226 meV for $Na_2(CB_9H_{10})(CB_{11}H_{12})$ [20] and ~450 meV for Na-7-$CB_{10}H_{13}$ [23]). Such a behavior is not expected in terms of the Nernst-Einstein equation. The reasons for this discrepancy are not yet clear. Similar discrepancies between the activation energies for the cation jump rates and the activation energies derived from conductivity measurements are typical of nanocrystalline ionic conductors [41]; they were also reported previously for a number of hydroborates, including $Na_2B_{10}H_{10}$ [3], $LiCB_{11}H_{12}$ and $NaCB_{11}H_{12}$ [13], $LiCB_9H_{10}$ and $NaCB_9H_{10}$ [5]. The higher activation energies for the measured conductivity may presumably be attributed to the effects of large-scale inhomogeneities (such as grain boundaries) [3].

4. Conclusions

Our pulsed-field-gradient spin-echo experiments have revealed the exceptionally fast Na^+ diffusivity in the mixed-anion *closo*-$Na_2(CB_9H_{10})(CB_{11}H_{12})$ over the temperature range of 298–403 K and in *nido*-Na-7-$CB_{10}H_{13}$ over the range of 320–403 K. These experiments represent the first direct measurements of Na^+ diffusion coefficients in complex hydrides. The measured diffusion coefficients are found to follow the Arrhenius behavior with the activation energies of 118(1) meV for $Na_2(CB_9H_{10})(CB_{11}H_{12})$ and 134(3) meV for Na-7-$CB_{10}H_{13}$. It should be noted that, for both compounds, the values of the activation energies for Na^+ diffusion coefficients are in reasonable agreement with the corresponding values for Na^+ jump rates, as derived from the ^{23}Na spin-lattice relaxation rate measurements. For $Na_2(CB_9H_{10})(CB_{11}H_{12})$, the room-temperature Na^+ conductivity σ estimated from the diffusivity data on the basis of Nernst-Einstein equation is consistent with the measured room-temperature conductivity value, which is higher than that of any known solid Na-ion or Li-ion conductor. However, in contrast to expectations based on Nernst-Einstein equation, for both compounds the activation energies for Na^+ diffusion coefficients appear to be lower than those for the experimental σT product.

The analysis of the measured ^{1}H and ^{23}Na spin-lattice relaxation rates for Na-7-$CB_{10}H_{13}$ has shown that the transition from the low-T ordered phase to the high-T disordered phase occurring near 320 K is accompanied by the abrupt increase in both the reorientational jump rate of $[CB_{10}H_{13}]^-$ anions and the diffusive jump rate of Na^+ cations. In this respect, the dynamical properties of this *nido*-type compound resemble those of *closo*-type hydroborates [8,9,11]. The activation energies for anion reorientations derived from the ^{1}H spin-lattice relaxation data are 330(20) meV for the ordered phase and 219(5) meV for the disordered phase. The activation energies for Na^+ diffusive jumps found from the ^{23}Na spin-lattice relaxation results are 320(9) meV for the ordered phase and 116(7) meV for the disordered phase. It should be noted that *a priori* it is not evident that a *nido*-type anion $[CB_{10}H_{13}]^-$ can participate in the fast reorientational motion, since the geometry of this anion is quite complex (see Fig. 1a). Our experimental results are consistent with fast reorientations of this anion both in the ordered phase (^{1}H NMR) and in the disordered phase (^{1}H NMR and quasielastic neutron scattering). Information on the mechanisms of reorientations can, in principle, be obtained from QENS experiments. In the limited Q range of our present QENS measurements, the elastic incoherent structure factor results for the disordered phase appear to be consistent with the model of uniaxial reorientations around the five-fold symmetry axis of the boron frame. However, additional high-Q measurements are required to clarify the mechanism of reorientations.

CRediT authorship contribution statement

A.V. Skripov: Supervision, Writing - original draft. **G. Majer:** Investigation, Writing - review & editing. **O.A. Babanova:** Investigation, Software, Formal analysis. **R.V. Skoryunov:** Investigation, Visualization. **A.V. Soloninin:** Investigation, Methodology, Validation. **M. Dimitrievska:** Investigation, Formal analysis. **T.J. Udovic:** Methodology, Writing - review & editing.

Declaration of competing interest

The authors declare that they have no known competing financial interests or personal relationships that could have appeared to influence the work reported in this paper.

Acknowledgments

This work was performed within the assignment of the Russian federal scientific program “Function” No. AAAA-A19-119012990095-0, supported in part by the Russian Foundation for Basic Research (Grant. No. 19-03-00133). A.V. Skripov is grateful to the Alexander von Humboldt Foundation for financial support of his research visit to Max-Planck-Institute for Intelligent Systems. M.D. gratefully acknowledges support from the US DOE Office of Energy Efficiency, Fuel Cell Technologies Office, under Contract No. DE-AC36-08GO28308.

Appendix A. Supplementary data

Supplementary data related to this article can be found at https://doi.org/10.1016/j.jallcom.2020.156781.

References

[1] B.R.S. Hansen, M. Paskevicius, H. Li, E. Akiba, T.R. Jensen, Metal boranes: progress and applications, Coord. Chem. Rev. 323 (2016) 60–70.

[2] T.J. Udovic, M. Matsuo, A. Unemoto, N. Verdal, V. Stavila, A.V. Skripov, J.J. Rush, H. Takamura, S. Orimo, Sodium superionic conduction in $Na_2B_{12}H_{12}$, Chem. Commun. 50 (2014) 3750–3752.

[3] T.J. Udovic, M. Matsuo, W.S. Tang, H. Wu, V. Stavila, A.V. Soloninin, R.V. Skoryunov, O.A. Babanova, A.V. Skripov, J.J. Rush, A. Unemoto, H. Takamura, S. Orimo, Exceptional superionic conductivity in disordered sodium decahydro-*closo*-decaborate, Adv. Mater. 26 (2014) 7622–7626.

[4] W.S. Tang, A. Unemoto, W. Zhou, V. Stavila, M. Matsuo, H. Wu, S. Orimo, T.J. Udovic, Unparalleled lithium and sodium superionic conduction in solid electrolytes with large monovalent cage-like anions, Energy Environ. Sci. 8 (2015) 3637–3645.

[5] W.S. Tang, M. Matsuo, H. Wu, V. Stavila, W. Zhou, A.A. Talin, A.V. Soloninin, R.V. Skoryunov, O.A. Babanova, A.V. Skripov, A. Unemoto, S. Orimo, T.J. Udovic, Liquid-like ionic conduction in solid lithium and sodium monocarba-*closo*-decaborates near or at room temperature, Adv. Energy Mater. 6 (2016) 1502237.

[6] K. Yoshida, T. Sato, A. Unemoto, M. Matsuo, T. Ikeshoji, T.J. Udovic, S. Orimo, Fast sodium ionic conduction in $Na_2B_{10}H_{10}$-$Na_2B_{12}H_{12}$ complex hydride and application to a bulk-type all-solid-state battery, Appl. Phys. Lett. 110 (2017) 103901.

[7] S. Kim, H. Oguchi, N. Toyama, T. Sato, S. Takagi, T. Otomo, D. Arunkumar, N. Kuwata, J. Kawamura, S. Orimo, A complex hydride lithium superionic conductor for high-energy-density all-solid-state lithium metal batteries, Nat. Commun. 10 (2019) 1081.

[8] L. Duchêne, A. Remhof, H. Hagemann, C. Battaglia, Status and prospects of hydroborate electrolytes for all-solid-state batteries, Energy Storage Mater. 25 (2020) 782–794.

[9] S.H. Payandeh, R. Asakura, P. Avramidou, D. Rentsch, Z. Łodziana, R. Černý, A. Remhof, C. Battaglia, *Nido*-borate/*closo*-borate mixed-anion electrolytes for all-solid-state batteries, Chem. Mater. 32 (2020) 1101–1110.

[10] A.V. Skripov, O.A. Babanova, A.V. Soloninin, V. Stavila, N. Verdal, T.J. Udovic, J.J. Rush, Nuclear magnetic resonance study of atomic motion in $A_2B_{12}H_{12}$ (A = Na, K, Rb, Cs): anion reorientations and Na^+ mobility, J. Phys. Chem. C 117 (2013) 25961–25968.

[11] N. Verdal, J.-H. Her, V. Stavila, A.V. Soloninin, O.A. Babanova, A.V. Skripov, T.J. Udovic, J.J. Rush, Complex high-temperature phase transitions in $Li_2B_{12}H_{12}$ and $Na_2B_{12}H_{12}$, J. Solid State Chem. 212 (2014) 81–90.

[12] N. Verdal, T.J. Udovic, V. Stavila, W.S. Tang, J.J. Rush, A.V. Skripov, Anion reorientations in the superionic conducting phase of $Na_2B_{12}H_{12}$, J. Phys. Chem. C 118 (2014) 17483–17489.

[13] A.V. Skripov, R.V. Skoryunov, A.V. Soloninin, O.A. Babanova, W.S. Tang, V. Stavila, T.J. Udovic, Anion reorientations and cation diffusion in LiCB11H12 and NaCB11H12: 1H, 7Li, and 23Na NMR studies, J. Phys. Chem. C 119 (2015) 26912–26918.

[14] A.V. Soloninin, M. Dimitrievska, R.V. Skoryunov, O.A. Babanova, A.V. Skripov, W.S. Tang, V. Stavila, T.J. Udovic, Comparison of anion reorientational dynamics in MCB_9H_{10} and $M_2B_{10}H_{10}$ (M = Li, Na) via nuclear magnetic resonance and quasielastic neutron scattering studies, J. Phys. Chem. C 121 (2017) 1000–1012.

[15] Z. Lu, F. Ciucci, Structural origin of the superionic Na conduction in $Na_2B_{10}H_{10}$ *closo*-borates and enhanced conductivity by Na deficiency for high performance solid electrolyte, J. Mater. Chem. 4 (2016) 17740–17748.

[16] J.B. Varley, K. Kweon, P. Mehta, P. Shea, T.W. Heo, T.J. Udovic, V. Stavila, B.C. Wood, Understanding ionic conductivity trends in polyborane solid electrolytes from *ab initio* molecular dynamics, ACS Energy Lett. 2 (2017) 250–255.

[17] K. Kweon, J.B. Varley, P. Shea, N. Adelstein, P. Mehta, T.W. Heo, T.J. Udovic, V. Stavila, B.C. Wood, Structural, chemical, and dynamical frustration: origins of superionic conductivity in *closo*-borate solid electrolytes, Chem. Mater. 29 (2017) 9142–9153.

[18] M. Dimitrievska, P. Shea, K.E. Kweon, M. Bercx, J.B. Varley, W.S. Tang, A.V. Skripov, V. Stavila, T.J. Udovic, B.C. Wood, Carbon incorporation and anion dynamics as synergistic drivers for ultrafast diffusion in superionic $LiCB_{11}H_{12}$ and $NaCB_{11}H_{12}$, Adv. Energy Mater. 6 (2018) 1703422.

[19] W.S. Tang, M. Matsuo, H. Wu, V. Stavila, A. Unemoto, S. Orimo, T.J. Udovic, Stabilizing lithium and sodium fast-ion conduction in solid polyhedral-borate salts at device-relevant temperatures, Energy Storage Mater. 4 (2016) 79–83.

[20] W.S. Tang, K. Yoshida, A.V. Soloninin, R.V. Skoryunov, O.A. Babanova, A.V. Skripov, M. Dimitrievska, V. Stavila, S. Orimo, T.J. Udovic, Stabilizing superionic-conducting structures via mixed-anion solid solutions of monocarba-*closo*-borate salts, ACS Energy Lett. 1 (2016) 659–664.

[21] L. Duchêne, R.-S. Kühnel, D. Rentsch, A. Remhof, H. Hagemann, C. Battaglia, A highly stable sodium solid-state electrolyte based on a dodeca/deca-borate equimolar mixture, Chem. Commun. 53 (2017) 4195–4198.

[22] M. Brighi, F. Murgia, Z. Łodziana, P. Schouwink, A. Wołczyk, R. Černý, A mixed anion hydroborate/carba-hydroborate as a room temperature Na-ion solid electrolyte, J. Power Sources 404 (2018) 7–12.

[23] W.S. Tang, M. Dimitrievska, V. Stavila, W. Zhou, H. Wu, A.A. Talin, T.J. Udovic, Order-disorder transitions and superionic conductivity in the sodium *nido*-undeca(carba)borates, Chem. Mater. 29 (2017) 10496–10509.

[24] A.V. Skripov, A.V. Soloninin, O.A. Babanova, R.V. Skoryunov, Nuclear magnetic resonance studies of atomic motion in borohydride-based materials: fast anion reorientations and cation diffusion, J. Alloys Compd. 645 (2015) S428–S433.

[25] E.O. Stejskal, J.E. Tanner, Spin diffusion measurements: spin echos in the presence of a time-dependent field gradient, J. Chem. Phys. 42 (1965) 288–292.

[26] P. Stilbs, Fourier transform pulsed-gradient spin-echo studies of molecular diffusion, Prog. Nucl. Magn. Reson. Spectrosc. 19 (1987) 1–45.

[27] W.S. Price, NMR Studies of Translational Motion – Principles and Applications, University Press, Cambridge, UK, 2009.

[28] P.T. Callaghan, Translational Dynamics and Magnetic Resonance – Principles of Pulsed Gradient Spin Echo NMR, University Press, Oxford, UK, 2011.

[29] A.V. Soloninin, R.V. Skoryunov, O.A. Babanova, A.V. Skripov, M. Dimitrievska, T.J. Udovic, Comparison of anion and cation Dynamics in a carbon-substituted closo-hydroborate salt: 1H and 23Na NMR studies of solid-solution Na2(CB9H10)(CB11H12), J. Alloys Compd. 800 (2019) 247–253.

[30] The Mention of All Commercial Suppliers in This Paper Is for Clarity and Does Not Imply the Recommendation or Endorsement of These Suppliers by NIST.

[31] D. Burstein, Stimulated echos: description, applications, practical hints, Concepts Magn. Reson. 8 (1996) 269–278.

[32] J.R.D. Copley, J.C. Cook, The disk chopper spectrometer at NIST: a new instrument for quasielastic neutron scattering studies, Chem. Phys. 292 (2003) 477–485.

[33] A. Abragam, The Principles of Nuclear Magnetism, Clarendon Press, Oxford, 1961.

[34] M. Bée, Quasielastic Neutron Scattering, Principles and Applications in Solid State Chemistry, Biology and Materials Science, Adam Hilger, Bristol, UK, 1988.

[35] R. Hempelmann, Quasielastic Neutron Scattering and Solid State Diffusion, Clarendon Press, Oxford, UK, 2000.

[36] W.S. Price, P. Kuchel, Effect of nonrectangular field gradient pulses in the Stejskal and Tanner (diffusion) pulse sequence, J. Magn. Reson. 94 (1991) 133–139.

[37] G. Majer, K. Zick, Accurate and absolute diffusion measurements of rhodamine 6G in low-concentration aqueous solutions by the PGSE-WATERGATE sequence, J. Chem. Phys. 142 (2015) 164202.

[38] A.V. Skripov, M. Pionke, O. Randl, R. Hempelmann, Quasielastic neutron scattering study of hydrogen motion in C14- and C15-type $ZrCr_2H_x$, J. Phys. Condens. Matter 11 (1999) 1489–1502.

[39] U. Eberle, G. Majer, A.V. Skripov, V.N. Kozhanov, NMR studies of hydrogen diffusion in the hydrogen-stabilized Laves-phase compound C15-$HfTi_2H_x$, J. Phys. Condens. Matter 14 (2002) 153–164.

[40] A.V. Skripov, Hydrogen diffusion in Laves-phase compounds, Defect Diffusion Forum 224–225 (2003) 75–92.

[41] P. Heitjans, S. Indris, Diffusion and ionic conduction in nanocrystalline ceramics, J. Phys. Condens. Matter 15 (2003) R1257–R1289.